ISSN 1995-0802, Lobachevskii Journal of Mathematics, 2025, Vol. 46, No. 5, pp. 2406–2414. © Pleiades Publishing, Ltd., 2025.

New Possibilities of the Fourier Transformation: How to Describe an Arbitrary Frequency-Phase Modulated Signal?

R. R. Nigmatullin[1]*, A. A. Litvinov[1,2], and S. I. Osokin[2]*****

(Submitted by A. M. Elizarov)

[1] *Tupolev Kazan National Research Technical University, Radioelectronics and Informative Measurements Technics Department, Kazan, 420111 Russia*

[2] *Kazan Federal University, Institute of Information Technologies and Intellectual Systems, Kazan, 420111 Russia*

Received January 18, 2025; revised March 25, 2025; accepted April 10, 2025

Abstract—In this paper, the authors found a transformation that is valid for any arbitrary signal. This transformation is strictly periodical and, therefore, it allows to apply the ordinary F-transformation for the fitting of the transformed signal. The most interesting application (in accordance with the author's opinion) is the fitting of the frequency-phase modulated signals that located actually inside the found transformation. This new transformation will be useful for application of the responses of different complex systems when a particular model is absent. As available data, we consider cosmic microwave background data (CMB) associated with the background temperature fluctuations near $T = 2.725$ K. These electro-magnetic (EM) fluctuations of the early Universe were measured at the wide frequency range 30–857 GHz. In this paper, we analyzed the measured data at 353 GHz corresponding to the taken zero pixels. Other details are described in the second section of the paper. This squared matrix corresponding to the measured data contains 2047 lines $\times$ 2047 columns. If one considers each column as frequency-phase modulated signal, then amplitude-frequency response can be evaluated with the help of F-transformation that has the period equals 2π that is valid for any analyzed random signal. These "universal" behavior allows to fit a wide set of random signals and compare them with each other in terms of their amplitude-frequency responses (AFR). Concluding the abstract, one can say that these new possibilities of the traditional F-analysis will serve as a common tool in the armory of the methods used by researchers in the data processing area.

2010 Mathematics Subject Classification: 42A38, 42B10, 35A22, 65P99

DOI: 10.1134/S1995080225605636

Keywords and phrases: *Fourier transformation (F-transformation), Fourier analysis (F-analysis), Fourier series, cosmic microwave background data, electro-magnetic fluctuations, amplitude-frequency responses, fitting of the frequency-phase modulated signals*

1. INTRODUCTION AND FORMULATION OF THE PROBLEM

Everybody knows the basic drawback of the traditional F-transformation. It lies in supposition that any digital random signal is periodical, i.e.,

$$Sg(t+T) = Sg(t). \tag{1}$$

Here $Sg(t)$ defines an arbitrary random signal, T is a period coinciding with $\mathrm{Range}(t)$ ($T \approx Rg(t)$). The last definition $\mathrm{Range}(t) = \max t - \min t$ determines the length of the $Sg(t)$ analyzed. In many cases, this supposition is unprovable and, therefore, many researches try to overcome this supposition.

*E-mail: renigmat@gmail.com

**E-mail: litvinov85@gmail.com

***E-mail: s.osokin@it.kfu.ru

If we want to replace the pure periodic signal by some aperiodic copy, then one will have the following problem. The discrete aperiodic signal fitting issue cannot be resolved by the integral Fourier transform of aperiodic signals; hence, it cannot be used for prediction an aperiodic signal outside of the specified time window interval. The discrete representations of many analog signals play an important role in their processing. They contain relevant information related to the properties of the signals and admit their further processing [1]. In the conventional scheme, signals can be presented in the form of Taylor–Maclaurin, Dirichlet, Laurent, Legendre, Padé, Prony, and Fourier series. We would like to stress here that these decomposition series is used without any mathematical justification. The classical Fourier series (FS) is a simple and frequently used tool in the signal processing area. However, the FS does not identify both subharmonic and interharmonic components of the given signal and, in many situations, it has serious drawbacks [2–5]. The proposed method allows the limitations of the Fourier analysis to be overcome. The Fourier analysis is based on time-frequency methods [6] that were used in the last few decades, namely the fractional [7–9], short time [10–12], windowed FT [13, 14], Gabor [15–17], wavelet [18–20], Hilbert–Huang [21–23], and Fourier–Bessel transformations [24, 25], and even decomposition over empirical modes [26]. These references prove that there are many different approximations for overcoming the basic drawback (1). However, attentive analysis allows to formulate the following problem. Is there universal transformation of an initial signal that allows to transform of it to another digital signal having strictly the period 2π. Really, if one can write the following relationship

$$Sg(t) = a\cos F(t) + b \tag{2}$$

and start to analyze instead of the initial function $Sg(t)$ the argument $F(t)$ of the cosine function, we obtain the desired result. The function $F(t)$ represents the combined frequency-phase modulated signal and provides the desired interval $[-1, 1]$ for $\cos F(t)$, while the argument $F(t)$ falls within the interval $[0, \pi]$. Therefore, the final result for the decomposition of any signal keeps the previous form (2) if one adds to it the decomposition of $F(t)$ by the fitting function $Yft(t, K)$ in the form final segment of the F-series

$$F(t) \cong Yft(t, K) = Ph_0 + \sum_{k=1}^{K} \left[Ac_k \cos(\Omega_k t) + As_k \sin(\Omega_k t)\right], \quad \Omega_k = 2, 3, \ldots, K. \tag{3}$$

Here one takes into account the property of $F(t) = F(t \pm \pi)$ that defines the semi-periodic function. Therefore, these two simple expressions (2) and (3) solve the problem of decomposition of any random function $Sg(t)$ to the segment of the F-series.

2. DESCRIPTION OF THE CMB DATA

The Planck satellite (PS) is the most recent European Satellite Airspace's space mission whose main objective was to measure the cosmic microwave background (CMB) temperature and polarization anisotropies, with an accuracy set only by the fundamental astrophysical limits. PS mapped the entire sky with angular resolutions from 31 to 5 arc/min, at nine frequency bands covering 30–857 GHz [27]. The analysis of CMB data led to our strongest constraints on the standard cosmological model parameters [28], on the inflation scenarios [29], and on the non-Gaussianity of the primordial cosmological perturbations [30]. The data analyzed in the paper are the CMB temperature fluctuations around the mean value 2,725 K measured by PS at the frequencies 353 GHz. For the analyzed frequencies, CMB temperature maps are provided by European Space Agency (ESA) in HEALPix (Hierarchical Equal Area isoLatitude Pixelization) [31] nested ordering format with $Nside = 2048$ (order $N = 11$). The HEALPix scheme allows dividing the sky into a number of pixels depending on the Nth side $= 2N$ parameter, where N is called the order. In the nested scheme, the sky is primarily ($N = 0$) divided into 12 pixels (primary pixels). For $N \geq 1$, each primary pixel is divided into $2N \times 2N$ secondary pixels [32]. ESA provided PS's data in one-dimensional array in which the position K corresponds to the K-index in the HEALPix nested scheme. This leads to the situation that adjacent values in the 1D array are not adjacent on the sky. Since this is a disadvantage when the data is to be treated as 1D or 2D temperature distributions, we reordered and arranged the data in 2D matrix format such that adjacent pixels in the matrix are also adjacent on the sky. We prepared this way the CMB measurements taken to individual frequencies 353 GHz and, therefore, finally, we obtained for data analysis the matrices containing 2047(lines)$\times$ 2047(columns) for each divided pixels (Pl=0,1,...,11).

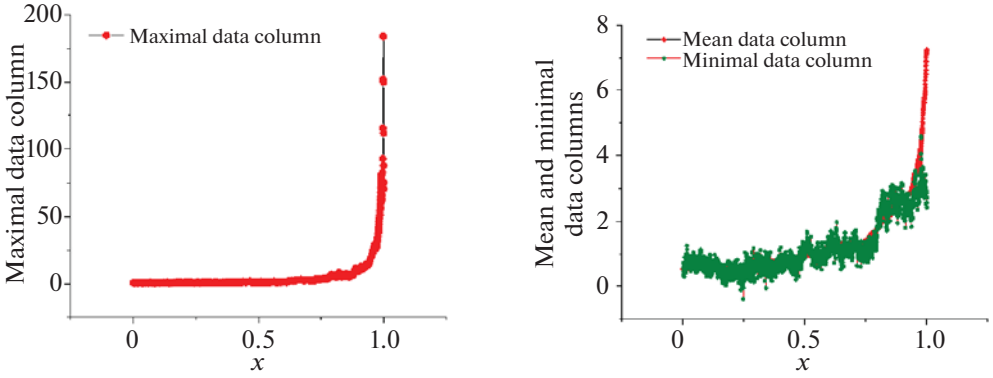

Fig. 1. On the left, we demonstrate the maximal file (corresponding to 2046 column) and, on the right, we demonstrate the mean file (shown by the connected red points) and minimal file corresponding to the 1321st column (shown by connected green points). The independent variable $x_j = j/N$ (corresponding to the sizeless temporal value $x = t$) is normalized to the unit value.

These matrixes were sent to one of the authors (RRN) for analysis by Prof. Dumitru Baleanu from Cosmic Airspace Institute from Bucharest (Romania). Because the sent data were remained extremely large, we chose for the further analysis only one data file with number of pixels Pl=0 (the file named—"pixel_00.txt" that forms the matrix $[\mathbf{M}_0] = 2047(\text{lines}) \times 2047(\text{columns})$).

3. DESCRIPTION OF THE PROCESSING PROCEDURE

Definitely, it is impossible to demonstrate all fitting functions ($S = 2047$) corresponding to the recorded signal and coinciding with each column. Having in mind the demonstration of new method, we choose only three basic curves corresponding to the maximal, mean and minimal curves, correspondingly. These curves increased in 10^3 times (for conveniences) are showed in Fig. 1.

Calculation of the arguments $Fq(t)(q = 0, 1, 2)$ from (2) for these curves located in the interval $(0, \pi)$ are shown in Fig. 2.

In order to find the AFR for these three curves it is convenient to use the NOCFASS (Non-Orthogonal Combined Fourier Analysis of the Smoothed Signals) [32]. This modified approach helps to decrease considerably the number of modes that depends essentially of the value of the final mode K. The value of K is determined by the value of the relative error that is calculated in turn from the expression

$$\text{Rel}Err(K) = \left[\frac{stdev(F(t) - Yft(t, K))}{mean|F(t)|}\right] \times 100\%. \tag{4}$$

The curves depicted in Fig. 2 are fitted by expression (2). The results are explained by Fig. 3.

For the fitting purposes it is sufficient to take small number of frequencies covering the interval [Vect, Vect + 200]. The final result is shown in Figs. 4 and 5. The amplitude-frequency response is given in Fig. 5.

In order to finish the fitting procedure, we demonstrate the transition from the fit of the argument $F_0(t)$ to the initial signal $Mex(t)_0$ on Fig. 6.

Approximate fitting function of the initial signal is defined by similar expression

$$Ex(t) = a\cos(Yft(t)) + b,$$

where the scaling parameters a and b are found as the slope and intercept, accordingly, from the central Fig. 6. In the same manner, one can fit the random curves depicted on the right Fig. 2. In order not to clutter the text with a large number of pictures, we will give only the main ones on Figs. 7 and 8.

If one compares the Amd_k for the curves $F_{0,1}(t)$ one can notice that they are completely different in spite of their initial similarity (see Figs. 9, 10, and 11).

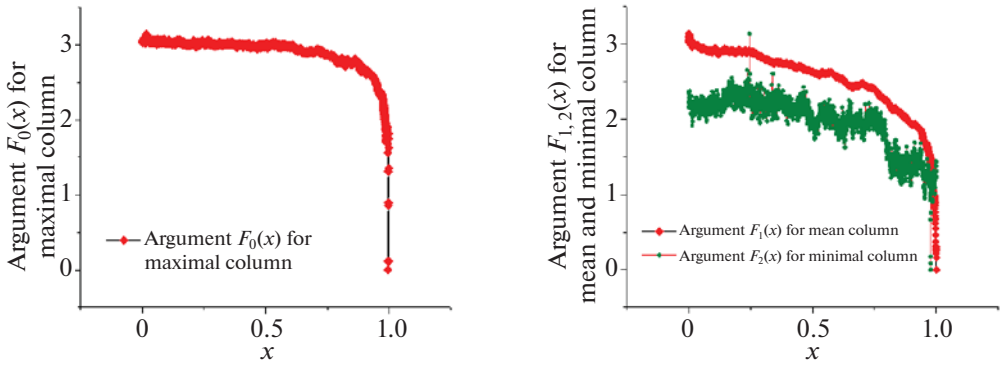

Fig. 2. On the left, we demonstrate the argument $F_0(t)$ of the cosine function for the maximal curve, on the right figure, we demonstrate the corresponding arguments for the mean curve $F_1(t)$ (connected by red points) and for the minimal curve $F_2(t)$ (shown by connected green points).

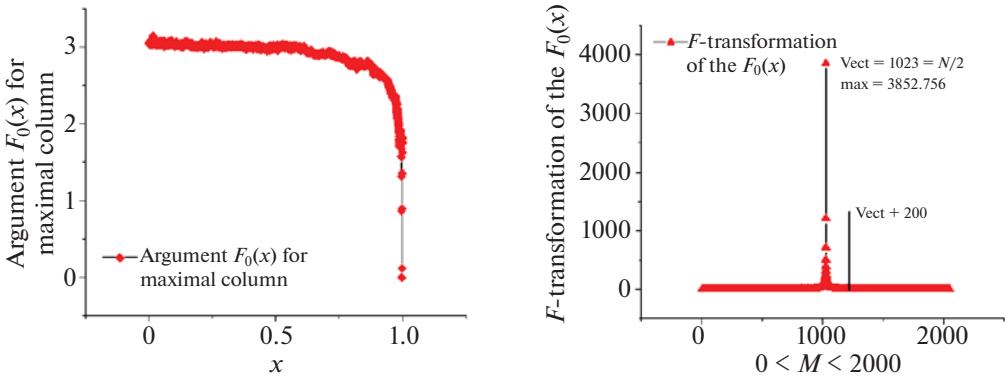

Fig. 3. On the right figure, we demonstrate the F-transformation of the curve $F_0(t)$ shifted to the center of the F-transformation using the angle π. Thanks to the shift of the conventional F-transformation to the π-angle one can see easily the resonance frequency at Vect $= 1023 = N/2$, with maximal value Fr $= 3852.756$ and other set of frequencies symmetrically located on both sides of the resonance curve. Solid black line on the right select the right boundary (Vect $+$ 200) of the frequencies that is sufficient for the fitting purposes.

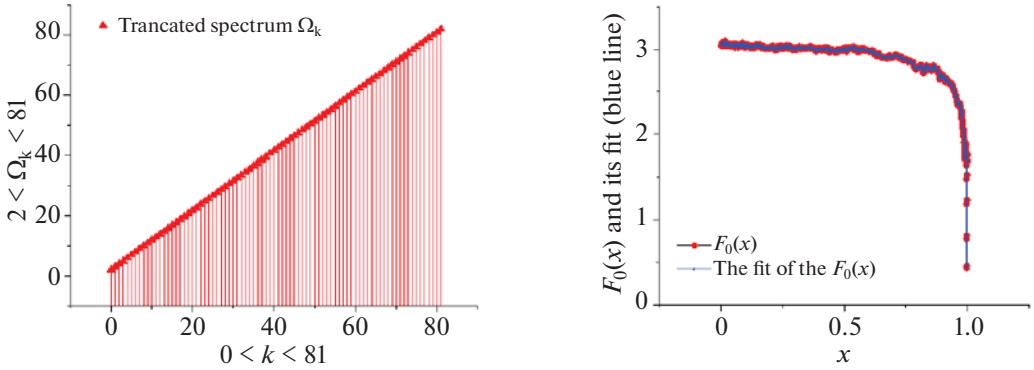

Fig. 4. The left figure demonstrates the truncated spectrum located in the interval [2] that is sufficient to provide the desired fit with the value of the relative error (defined by expression (4)) less than 1%. The fitting function $Yft(t)$ for the function $F_0(t)$ is shown on the right figure by the solid blue line. The accurate relative error values are collected in the Table 1.

4. RESULTS AND DISCUSSION

The new modification of the traditional F-transformation opens new perspectives for the fitting practically a wide set of random functions. One can state that any random function has its own AFR.

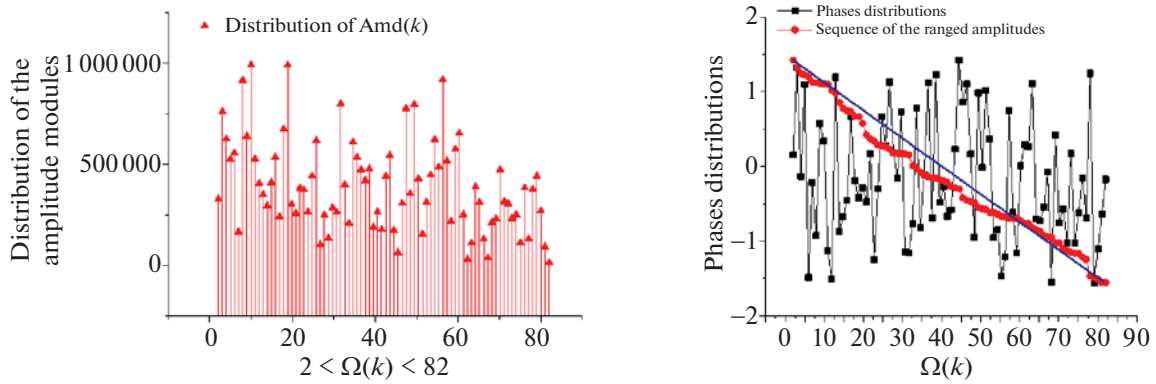

Fig. 5. On the left figure, we demonstrate the modulus of the amplitudes $Amd_k = \sqrt{Ac_k^2 + As_k^2}$, while the right figure describes the phase distribution $Phase_k = \tan^{-1}(As_k/Ac_k)$ for the function $F_0(x)$. The solid straight line shown on the right figure corresponds to the sequence of the range amplitudes (SRA) of ordered phases. It is easy to notice that is close to the segment of the straight line shown by bold black line. This fact signifies that the phase distribution is almost uniform.

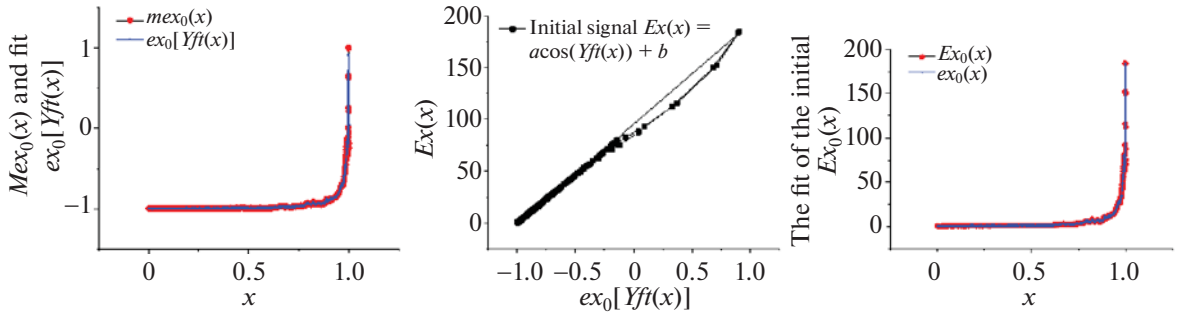

Fig. 6. These three figures demonstrate the fitting restoration of initial signal. On the left, we show the scaled function $mex_0(x) = \cos F_0(x)$ (connected red points) and its fit $ex_0(Yft(x))$ shown by blue solid line. In order to find the true scaling parameters, we use the central figure that helps to find the desired slope ($a = 92.167$) and intercept ($b = 92.347$). The final fitting function is shown in the right figure.

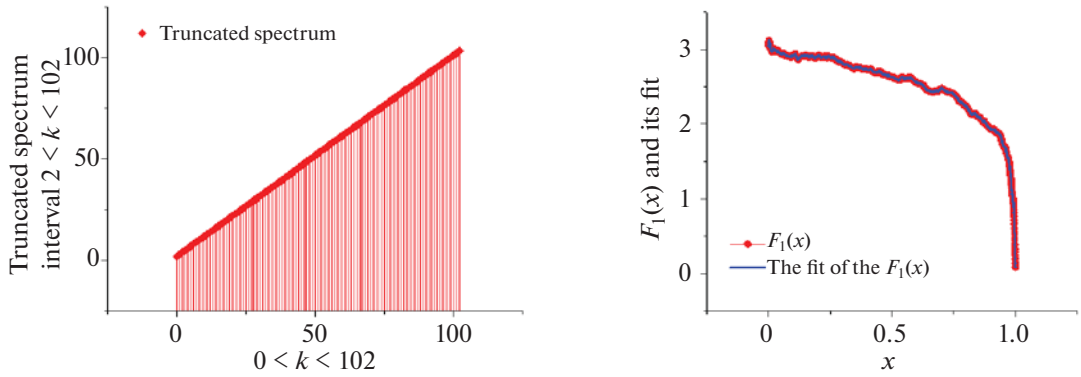

Fig. 7. The left figure demonstrates the truncated spectrum located in the interval [2] that is sufficient to provide the desired fit with the value of the relative error (defined by expression (4)) less than 1%. The fitting function $Yft(t)$ for the function $F_1(t)$ is shown on the right figure by the solid blue line. The accurate relative error values are collected in the Table 1.

This AFR located inside the cosine argument (see expressions (2) and (3)) and it gives actually the true spectrum for the frequency-phase modulated signals and the second spectrum for the amplitude modulated signals. Really, if the random signal has the following structure

$$Sg(t) = A(t)\cos Fr(t) \to a\cos F(t) + b,$$

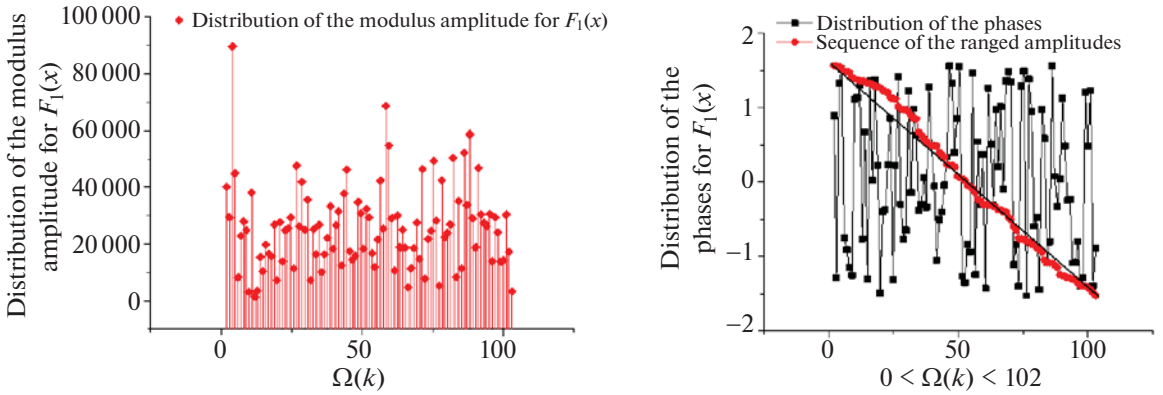

Fig. 8. On the left figure, we demonstrate the modulus of the amplitudes $Amd_k = \sqrt{Ac_k^2 + As_k^2}$, while the right figure describes the phase distribution $Phase_k = \tan^{-1}(As_k/Ac_k)$ for the argument $F_1(t)$. The solid straight line shown on the right figure corresponds to the sequence of the range amplitudes (SRA) for the ordered phases. It is easy to notice that is close to the segment of the straight line. This fact signifies again that the phase distribution is almost uniform.

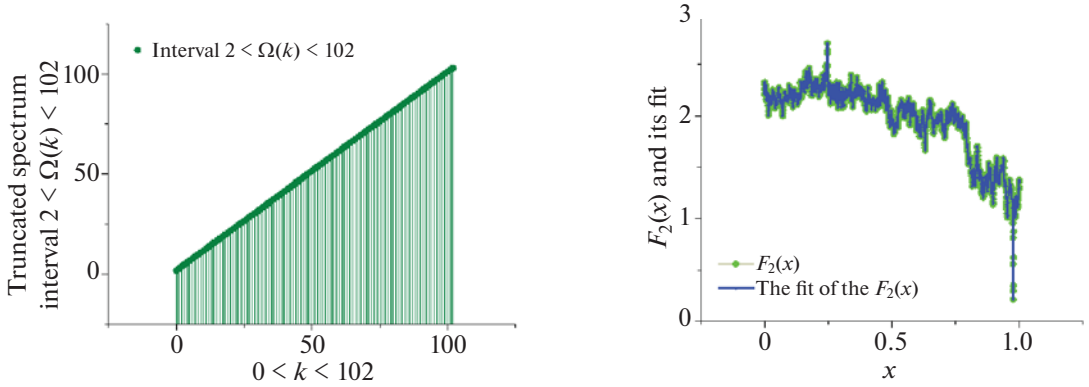

Fig. 9. The left figure demonstrates the truncated spectrum located in the interval [2] that is sufficient to provide the desired fit with the value of the relative error (defined by expression (4)) less than 1%. The fitting function $Yft(t)$ for the function $F_2(t)$ is shown on the right figure by the solid blue line. The accurate relative error values are collected in the Table 1.

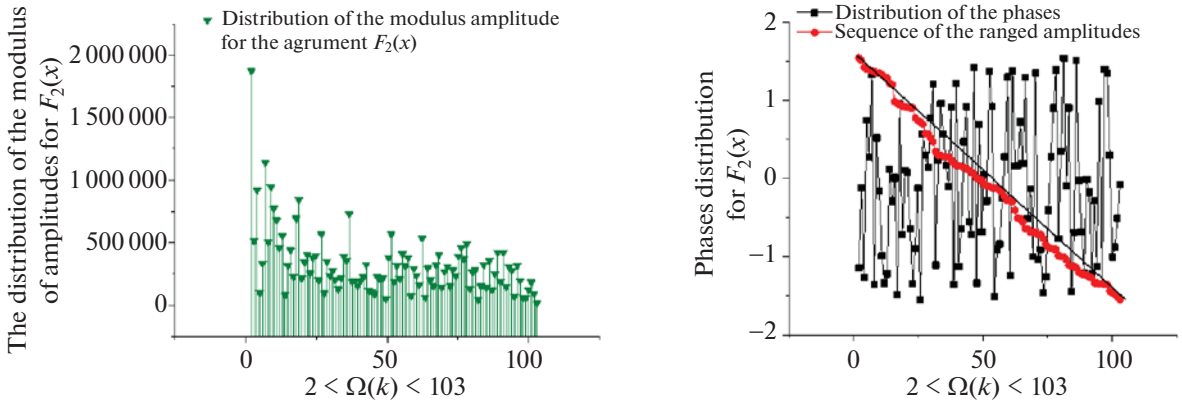

Fig. 10. On the left figure, we demonstrate the modulus of the amplitudes $Amd_k = \sqrt{Ac_k^2 + As_k^2}$, while the right figure describes the phase distribution $Phase_k = \tan^{-1}(As_k/Ac_k)$ for the argument $F_2(t)$. The solid straight line shown on the right figure corresponds to the sequence of the range amplitudes (SRA) for the ordered phases. It is easy to notice that is close to the segment of the straight line. This visual observation is repeated. This fact signifies again that the phase distribution is almost uniform.

then the first part of the random signal $Sg(t)$ includes all three types of possible modulations (amplitude, frequency and phase ones). The transformation used in this paper is applicable accurately for two types of modulations (frequency and phase ones), while for amplitude modulations it can be considered as approximate. Nevertheless, the AFR calculated for the function $F(t)$ can be considered as useful

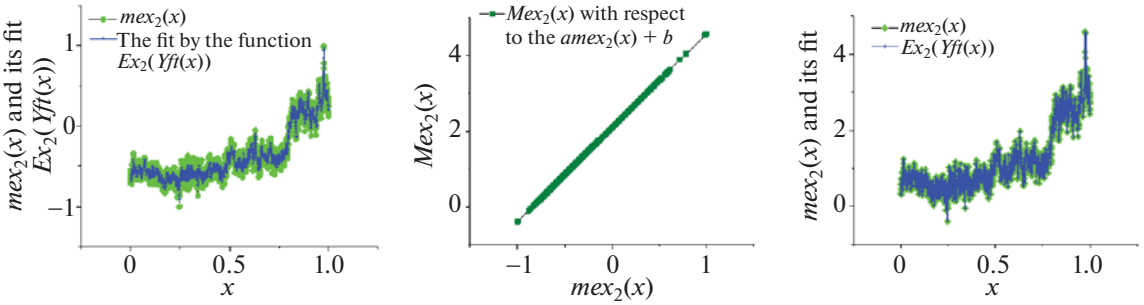

Fig. 11. These three figures demonstrate the fitting restoration of initial signal. On the left, we show the scaled function $mex_2(t) = \cos F_2(t)$ (connected by the light green points) and its fit $Ex_2(Yft(t))$ shown by blue solid line. In order to find the true scaling parameters, we use the central figure that helps to find the desired slope $a = 2.486$ and intercept ($b = 2.096$). The final fitting function for the function $Mex_2(t)$ is shown in the right figure. We placed these figures for the "noisy"argument distribution $F_2(t)$ in order to stress the accuracy of the used F-modification. Initially $Mex_2(t)$ depicted in Fig. 1 looks as a random function and the select an appropriate fitting function is not an easy problem. The approach proposed in this paper solves this problem by nontraditional way that is clearly seen in Fig. 11.

secondary spectrum in analysis and the fitting of different random signals with amplitude modulation. If the amplitude modulation is absent then the relationship (2) becomes the single and accurate. The previous formula (2) admits the following generalization if $Sg(t)$ is presented in the form of one mode as

$$Sg(t) = A\cos F(t) + B\sin F(t),$$

where the constants A and B are supposed to be known. Using simple algebraic manipulations one can find easily the argument $F(t)$

$$F(t) = \cos^{-1}\left(\frac{Sg(t)}{\sqrt{A^2+B^2}}\right) + \tan^{-1}\frac{B}{A}. \tag{5}$$

Therefore, expression (5) generalizes the previous expressions and increases the application boundaries of the proposed F-transformation.

In conclusion, we would like to say a few words about the novelty of the proposed method. As we know, the traditional Fourier transform is based on the assumption that there exists a certain period for which the following relation $Sg(t+T) = Sg(t)$ holds (see formula (1)). But the reality is that most of the signals are random and this relation is not fulfilled. The authors of the article asked the question: is there such a nonlinear transformation of a random signal that for the transformed signal this relation is fulfilled exactly? Such a transformation has been found and, as it turned out, it appears as the argument $F(t)$ of the periodic function in formula (2). Hence, strictly speaking, it is not the random function itself, but its argument $F(t)$, which is included in the cosine function. This function is periodic and satisfies the decomposition requirements accepted for discrete periodic functions. But, due to nonlinear coupling (see formula (2)), the spectrum will differ significantly from the generally accepted Fourier series expansion. To the decomposition of the function $F(t)$, we can apply NOCFASS (see reference [33]) by modifying the Fourier series, which actually shifts the entire Fourier spectrum to the left by the angle π (see Fig. 3 and using a segment of the spectrum counted from the shifted one to the right (see Fig. 4, one can find the part of the frequency spectrum needed to fit the original random function $Sg(t)$ with an accuracy of a few percent. This is the novelty of the new approach, which has proved its effectiveness on the original relic radiation data given to one of the authors (RRN) of this paper.

Table 1. The basic fitting parameters that were used for the fitting purposes of the functions $F_p(t)$ ($p = 0, 1, 2$)

Function	F_{res}	Ph_0	RelErr(%)	K	a	b
$F_0(t)$	3832.756	0.282	0.112	81	92.1672	92.3473
$F_1(t)$	3433.559	0.619	0.092	103	3.3585	3.8223
$F_2(t)$	2679.794	0.902	0.087	103	2.4856	2.0961

Finishing this section let us highlight the basic points obtained in this paper.

1. For a random function $Sg(t)$ the pure periodic functions $F(t)$ was found.

2. This function $F(t)$ is connected by nonlinear way with the initial random signal.

3. The proposed approach solves a problem of the fitting of a wide class the frequency-phase modulated signals.

4. The approach will be useful especially for description of the responses of different complex systems as technical, financial, medical etc, when the simple model is absent.

ABBREVIATIONS AND NOTATION

AFR—amplitude-frequency responses; CMB—cosmic microwave background data; EM—electromagnetic; ESA—European Space Agency; FS—Fourier series; HEALPix—Hierarchical Equal Area isoLatitude Pixelization; NOCFASS—Non-Orthogonal Combined Fourier Analysis of the Smoothed Signals; PS—Planck satellite; SRA—sequence of the range amplitudes.

FUNDING

Two of us (RRN and AAL) declare that this work was done in the frame of the State program Priority 2030 (Kazan National Research Technical University).

CONFLICT OF INTEREST

The authors of this work declare that they have no conflicts of interest.

REFERENCES

1. A. Mertins, *Signal Analysis: Wavelets, Filter Banks, Time-Frequency Transforms and Applications* (Wiley, Chichester, UK, 1999).
2. F. Arecchi, R. Meucci, G. Puccioni, and J. Tredicce, "Experimental evidence of subharmonic bifurcations, multistability, and turbulence in a Q-switched gas laser," Phys. Rev. Lett. **49**, 1217–1220 (1982).
3. J. Chen, K. Chau, C. Chan, and Q. Jiang, "Subharmonics and chaos in switched reluctance motor drives," IEEE Trans. Energy Convers. **17**, 73–78 (2002).
4. W. Lauterborn and E. Cramer, "Subharmonic route to chaos observed in acoustics," Phys. Rev. Lett. **47**, 1445 (1981).
5. I. Wilden, H. Herzel, G. Peters, and G. Tembrock, "Subharmonics, biphonation, and deterministic chaos in mammal vocalization," Bioacoustics **9**, 171–196 (1998).
6. L. Cohen, *Time-Frequency Analysis,* Vol. 778 of *Prentice Hall Signal Processing Series* (Prentice Hall, NJ, 1995).
7. L. B. Almeida, "The fractional Fourier transform and time-frequency representations," IEEE Trans. Signal Process. **42**, 3084–3091 (1994).
8. E. Sejdić, I. Djurović, and L. Stanković, "Fractional Fourier transform as a signal processing tool: An overview of recent developments," Signal Process. **91**, 1351–1369 (2011).
9. X. Su, R. Tao, and X. Kang, "Analysis and comparison of discrete fractional Fourier transforms," Signal Process. **160**, 284–298 (2019).
10. M. Portnoff, "Time-frequency representation of digital signals and systems based on short-time Fourier analysis," IEEE Trans. Acoust. Speech Signal Process. **28**, 55–69 (1980).
11. S. Qian and D. Chen, "Joint time-frequency analysis," IEEE Signal Process. Mag. **16**, 52–67 (1999).
12. M. Li, Y. Liu, S. Zhi, T. Wang, and F. Chu, "Short-time Fourier transform using odd symmetric window function," J. Dyn. Monit. Diagn. **1**, 37–45 (2022).
13. P. Hlubina, J. Luňáêk, D. Ciprian, and R. Chlebus, "Windowed Fourier transform applied in the wavelength domain to process the spectral interference signals," Opt. Commun. **281**, 2349–2354 (2008).
14. Q. Kemao, "Windowed Fourier transform for fringe pattern analysis," Appl. Opt. **43**, 2695–2702 (2004).
15. S. Qian and D. Chen, "Discrete Gabor transform," IEEE Trans. Signal Process. **41**, 2429–2438 (1993).
16. J. Yao, P. Krolak, and C. Steele, "The generalized Gabor transform," IEEE Trans. Image Process **4**, 978–988 (1995).

17. Z. Zhao, R. Tao, G. Li, and Y. Wang, "Clustered fractional Gabor transform," Signal Process. **166**, 107240 (2020).
18. S. Mallat, *A Wavelet Tour of Signal Processing,* 3rd ed. (Academic, Burlington, MA, 1999).
19. R. Yan, R. X. Gao, and X. Chen, "Wavelets for fault diagnosis of rotary machines: A review with applications," Signal Process. **96**, 1–15 (2014).
20. A. Kumar, "Wavelet signal processing: A review for recent applications," Int. J. Eng. Tech. **6**, 12 (2020).
21. Z. K. Peng, W. T. Peter, and F. L. Chu, "A comparison study of improved Hilbert-Huang transform and wavelet transform: Application to fault diagnosis for rolling bearing," Mech. Syst. Signal Process. **19**, 974–988 (2005).
22. A. I. Zayed, "Hilbert transform associated with the fractional Fourier transform," IEEE Signal Process. Lett. **5**, 206–208 (1998).
23. U. B. De Souza, J. P. L. Escola, and L. da Cunha Brito, "A survey on Hilbert–Huang transform: Evolution, challenges and solutions," Digit. Signal Process. **120**, 103292 (2022).
24. A. Bhattacharyya, L. Singh, and R. B. Pachori, "Fourier–Bessel series expansion based empirical wavelet transform for analysis of non-stationary signals," Digit. Signal Process. **78**, 185–196 (2018).
25. P. K. Chaudhary, V. Gupta, and R. B. Pachori, "Fourier-Bessel representation for signal processing, A review," Digit. Signal Process. **135**, 103938 (2023).
26. N. E. Huang, Z. Shen, S. R. Long, M. C. Wu, H. H. Shih, Q. Zheng, N. C. Yen, C. C. Tung, and H. H. Liu, "The empirical mode decomposition and the Hilbert spectrum for nonlinear and non-stationary time series analysis," Proc. R. Soc. London, Ser. A **454**, 903–995 (1998).
27. Z. Wu and N. E. Huang, "Ensemble empirical mode decomposition: A noise-assisted data analysis method," Adv. Adapt. Data Anal. **1**, 1–41 (2009).
28. Planck Collab., "Planck 2015 results I. Overview of products and scientific results," Astron. Astrophys. **594** (2016). https://doi.org/10.1051/0004-6361/201527101
29. Planck Collab., "Planck 2018 results I. Overview and the cosmological legacy of Planck," Astron. Astrophys. **641** (2020). https://doi.org/10.1051/0004-6361/201833880
30. Planck Collab., "Planck 2018 results X. Constraints on inflation," Astron. Astrophys. **641** (2020). https://doi.org/10.1051/0004-6361/201833887
31. Planck Collab., "Planck 2018 results IX. Constraints on primordial non-Gaussianity," Astron. Astrophys. **641** (2020). https://doi.org/10.1051/0004-6361/201935891
32. K. M. Gorsky et al., "HEALPix: A framework for high-resolution discretization and fast analysis of data distributed on the sphere," Astrophys. J. **622**, 759–771 (2005). https://doi.org/10.1086/427976
33. R. R. Nigmatullin, V. Alexandrov, P. Agarwal, Sh. Jain, and N. Ozdemir, "Description of multi-periodic signals generated by complex systems: NOCFASS – new possibilities of the Fourier analysis," Numer. Algebra, Control Optim. **14**, 1–19 (2024). https://doi.org/10.3934/naco.2022008